

This document is downloaded from DR-NTU, Nanyang Technological University Library, Singapore.

Title	Polaronic discontinuities induced by off-diagonal coupling
Author(s)	Zhang, Yuyu; Duan, Liwei; Chen, Qing-Hu; Zhao, Yang
Citation	Zhang, Y., Duan, L., Chen, Q., & Zhao, Y. (2012). Polaronic discontinuities induced by off-diagonal coupling. <i>The Journal of Chemical Physics</i> , 137(3), 034108-.
Date	2012
URL	http://hdl.handle.net/10220/9396
Rights	© 2012 American Institute of Physics. This paper was published in <i>The Journal of Chemical Physics</i> and is made available as an electronic reprint (preprint) with permission of American Institute of Physics. The paper can be found at the following official DOI: [http://dx.doi.org/10.1063/1.4733986]. One print or electronic copy may be made for personal use only. Systematic or multiple reproduction, distribution to multiple locations via electronic or other means, duplication of any material in this paper for a fee or for commercial purposes, or modification of the content of the paper is prohibited and is subject to penalties under law.

Polaronic discontinuities induced by off-diagonal coupling

Yuyu Zhang, Liwei Duan, Qinghu Chen, and Yang Zhao

Citation: *J. Chem. Phys.* **137**, 034108 (2012); doi: 10.1063/1.4733986

View online: <http://dx.doi.org/10.1063/1.4733986>

View Table of Contents: <http://jcp.aip.org/resource/1/JCPSA6/v137/i3>

Published by the [American Institute of Physics](#).

Additional information on *J. Chem. Phys.*

Journal Homepage: <http://jcp.aip.org/>

Journal Information: http://jcp.aip.org/about/about_the_journal

Top downloads: http://jcp.aip.org/features/most_downloaded

Information for Authors: <http://jcp.aip.org/authors>

ADVERTISEMENT



Goodfellow
metals • ceramics • polymers • composites
70,000 products
450 different materials
small quantities fast

www.goodfellowusa.com

Polaronic discontinuities induced by off-diagonal coupling

Yuyu Zhang,^{1,2} Liwei Duan,¹ Qinghu Chen,³ and Yang Zhao^{1,a)}

¹*Division of Materials Science, Nanyang Technological University, Singapore 639798, Singapore*

²*Center for Modern Physics, Chongqing University, Chongqing 400044, China*

³*Department of Physics, Zhejiang University, Hangzhou 310027, China*

(Received 28 April 2012; accepted 22 June 2012; published online 17 July 2012)

In this paper, we study a form of the Holstein molecular crystal model in which the influence of lattice vibrations on the transfers of electronic excitations between neighboring sites (off-diagonal coupling) is taken into account. Using the Toyozawa Ansatz and the Lanczos algorithm, the Holstein Hamiltonian with two types of off-diagonal coupling is studied focusing on a number of analyticity issues in the ground state. For finite-sized lattices and antisymmetric coupling, a sequence of discontinuities are found in the polaron energy dispersion, the size of the ground-state phonon cloud, and the linearized von Neumann entropy used to quantify the quantum entanglement between the exciton and the phonons in the ground state. Such behavior is accompanied by a shift of the ground-state crystal momentum from zero to nonzero values as the coupling strength is increased. In the thermodynamic limit, all discontinuities associated with antisymmetric coupling vanish except the one corresponding to the initial departure of the ground-state wavevector from the Brillouin zone center. For the case of symmetric off-diagonal coupling, a smooth crossover is found to exist in all parameters regimes. © 2012 American Institute of Physics. [<http://dx.doi.org/10.1063/1.4733986>]

I. INTRODUCTION

Exciton-phonon interactions give rise to polaronic features in optical and transport properties of organic materials.^{1,2} The process of polaron formation, which is centered on an electronic excitation interacting with lattice vibrations, is well described by the Holstein model.³ The commonly seen form of exciton-phonon coupling is the diagonal type, defined as a nontrivial dependence of the exciton site energy on phonon coordinates. Diagonal exciton-phonon coupling has been treated by quite a few numerical techniques^{4–12} revealing a smooth crossover transition from the weak- to strong-coupling regime. Despite being infrequently studied in early days, off-diagonal exciton-phonon coupling, which is defined as a nontrivial dependence of the exciton transfer integral on phonon coordinates, appears recently to garner increasing attention due to a surge of interest in the possible existence of nonanalyticities in models with phonon modulations of exciton tunneling between neighboring sites.^{13,14} An often-mentioned form of off-diagonal coupling is the Peierls-type coupling in the tight-binding Su-Schrieffer-Heeger (SSH) model,^{15–17} introduced to describe transport properties of 1D polyacetylene. Simultaneous presence of two types of coupling seems crucial to characterize solid-state excimers, where a variety of considerations point to a strong dependence of electronic tunneling upon certain coordinated distortions of neighboring molecules in the formation of bound excited states.^{18,19} Mishchenko and Nagaosa have shown that off-diagonal coupling allows coexistence of free and self-trapped states even in one spatial dimension.²⁰ It is claimed that their theory gives a consistent explanation to optical properties of quasi-one-dimensional compound A-PMDA consisting of alternating donor and accep-

tor molecules. It has also been proposed²¹ that off-diagonal coupling modulates the hopping integral of the Zhang-Rice singlet and the superexchange interaction, and is especially relevant in the low-doping regime of high-temperature superconductivity.

Our purpose here is to study the Holstein model with off-diagonal coupling focusing on a number of analyticity issues. Due to inherent difficulties in obtaining accurate solutions, off-diagonal coupling has not been adequately addressed in the literature.^{22,23} Recent studies by Zhao *et al.*^{5,24–29} using the Munn-Silbey approach, the Toyozawa Ansatz, and its generalization, the Global-Local Ansatz, were proven successful for a wide range of off-diagonal coupling strength, yielding polaron energy bands lower than those obtained previously for all crystal momenta.²⁸ In addition, polaron energy band minima were convincingly shown to be momentum-dependent. Such results were also corroborated by those from the dynamic coherent potential approximation (under the Hartree approximation).³⁰ Marchand *et al.*¹⁴ pointed out the existence of a sharp transition in the ground state in the SSH model encountered as one departs from the center of the Brillouin zone. Based primarily on variational calculations,³¹ an additional type of abrupt transitions at the zone center in the presence of off-diagonal coupling was also claimed. Since off-diagonal coupling can cause bandwidth fluctuations, it alone can generate hopping even in the absence of the transfer integral. Traditionally, discontinuities at the zone center near the self-trapping transition are attributed to insufficient sophistication of the variational wave functions.^{5,13,26,30} With the inclusion of off-diagonal coupling, however, contention still surrounds the existence of nonanalyticities in the Holstein model. In this work, we revisit the part of the polaron problem with off-diagonal exciton-phonon coupling, and address the analyticity issue, especially in finite-sized systems.

^{a)}Electronic mail: yzhao@ntu.edu.sg.

Quantum entanglement is currently being pursued vigorously in the studies of polaronic crossovers in particular^{13,32} and many-body quantum phase transitions in general,^{33,34} as it is hoped that entanglement measures may shed light upon drastic many-body effects near critical points. Our previous studies of the 1D Holstein polaron with simultaneous diagonal and off-diagonal exciton-phonon coupling have revealed that quantum entanglement between excitonic and phononic degrees of freedom exhibits abrupt changes with the increasing exciton-phonon coupling strength which allows one to effectively characterize both the small and large polaron regimes as well as the crossover in between.¹³ In this work, we use the von Neumann entropy to quantify entanglement between an exciton and its phonon cloud, and examine comprehensively abrupt changes in the ground state properties of the Holstein polaron characterized by the quantum entanglement.^{13,35} The von Neumann entropy employed here is a direct extension of the classical entropy concept in the field of quantum mechanics, which has been widely applied to quantify the quantum entanglement of two subsystems.

Exact diagonalization (ED) is an effective tool to study properties of the polaron on a lattice of limited size for both weak- and strong-coupling regimes³⁶ if the full quantum nature of phonons is taken into account. Earlier studies by ED have been performed on polaron models with diagonal exciton-phonon coupling on finite lattices.^{7,8,37,38} Detailed explorations of the influence of the off-diagonal coupling by ED were also carried out for small clusters, such as a six-site lattice.^{31,39} The Lanczos algorithm is used to diagonalize the Hamiltonian, a technique successfully employed for strong-correlated many-body systems.⁴⁰ Translational invariance has often been considered in order to simplify the calculation and analysis of large clusters. For larger lattice sizes, ED is replaced by a variational method based upon the Toyozawa Ansatz. Two sets of variational parameters, one for each constituting particle type in the exciton-phonon system, are included in the trial state, and for the most of the phase diagram, this Ansatz proves to be robust in describing the exciton-phonon correlations. This variational scheme which uses a relaxation iteration technique^{41,42} has earlier been shown to be rather efficient compared with numerical approaches demanding far more expensive computational resources.^{43,44} Notably, the Toyozawa Ansatz can deal with much larger clusters with respectable accuracy than ED.

The focus of this work is on the polaron energy band and entanglement properties of the ground state in the presence of antisymmetric and symmetric off-diagonal exciton-phonon coupling. We apply ED to lattices with up to 16 sites and the variational method to larger clusters. For the antisymmetric off-diagonal exciton-phonon coupling, numerically exact analysis reveals phase-transition-like behavior which drives the polaron ground-state energy band toward a bimodal structure with a nonzero ground-state crystal momentum. As a consequence, there is an abrupt jump of the ground state energy of the finite-size lattices with an increasing off-diagonal coupling strength, and phase transition occurs. We also discuss properties of the zero crystal momentum polaron state which may not be the ground state. In this case, the discontinuities disappear and no phase transition is expected.

The remainder of the paper is organized as follows. In Sec. II, the Holstein Hamiltonian with symmetric and antisymmetric off-diagonal coupling is introduced. In Sec. III, we describe briefly the ED method using the Lanczos algorithm and the variational approach using the Toyozawa Ansatz. Results obtained using the two methods are presented for antisymmetric off-diagonal coupling. In Sec. IV, we describe briefly the effect due to symmetric off-diagonal coupling. Conclusions are drawn in Sec. V.

II. THE MODEL HAMILTONIAN

The Holstein molecular crystal model which describes the interaction between the exciton and its phonon reservoir is given as

$$\hat{H} = \hat{H}^{\text{ex}} + \hat{H}^{\text{ex-ph}} + \hat{H}^{\text{ph}}, \quad (1)$$

where

$$\hat{H}^{\text{ex}} = -J \sum_n a_n^\dagger (a_{n+1} + a_{n-1}) \quad (2)$$

is the exciton Hamiltonian that depicts excitonic hopping between nearest neighboring sites with the transfer integral J . Here a_n (a_n^\dagger) is the exciton annihilation (creation) operator for the n th site. The phonon Hamiltonian \hat{H}^{ph} is given as

$$\hat{H}^{\text{ph}} = \sum_n \hbar\omega_0 b_n^\dagger b_n, \quad (3)$$

where b_n^\dagger creates an optical phonon of frequency ω_0 on site n . The Hamiltonian $\hat{H}^{\text{ex-ph}}$ describing the interactions between the exciton and the phonons includes both the exciton-phonon diagonal and off-diagonal coupling terms

$$\hat{H}^{\text{ex-ph}} = \hat{H}^{\text{diag}} + \hat{H}^{\text{o.d.}}. \quad (4)$$

The diagonal exciton-phonon coupling is defined as a nontrivial dependence of the exciton site energies (for simplicity here we set all the site energies to be 0) on the lattice coordinates \hat{X}_n ($\hat{X}_n \propto b_n^\dagger + b_n$), and the off-diagonal coupling, as a nontrivial dependence of the exciton transfer integral on the lattice coordinates \hat{X}_n .²⁵⁻²⁷ In this work, only linear exciton-phonon coupling is considered, although in its absence, higher order exciton-phonon interactions may be important.^{45,46} The linear diagonal coupling term can be written as

$$\hat{H}^{\text{diag}} = g\hbar\omega_0 \sum_n a_n^\dagger a_n (b_n^\dagger + b_n), \quad (5)$$

where g is a dimensionless diagonal coupling constant. In this paper, we set diagonal coupling parameter $g = 0$ and focus our attention on the influences of the off-diagonal exciton-phonon coupling $\hat{H}^{\text{o.d.}}$, which consists of antisymmetric off-diagonal coupling $\hat{H}^{\text{o.d.a}}$ and symmetric off-diagonal coupling $\hat{H}^{\text{o.d.s}}$, as shown below^{5,27,28}

$$\begin{aligned} \hat{H}^{\text{o.d.a}} = & \phi\hbar\omega_0 \sum_{nl} [a_n^\dagger a_{n+1} (b_l^\dagger + b_l) (\delta_{n+1,l} - \delta_{nl}) \\ & + a_n^\dagger a_{n-1} (b_l^\dagger + b_l) (\delta_{nl} - \delta_{n-1,l})], \end{aligned} \quad (6)$$

$$\hat{H}^{\text{o.d.s}} = \phi \hbar \omega_0 \sum_{nl} \left[a_n^\dagger a_{n+1} (b_l^\dagger + b_l) (\delta_{n+1,l} + \delta_{nl}) + a_n^\dagger a_{n-1} (b_l^\dagger + b_l) (\delta_{nl} + \delta_{n-1,l}) \right], \quad (7)$$

where ϕ is a dimensionless parameter describing the strength of off-diagonal coupling. It is noted that the definition of ϕ above differs from that in our previous publications^{25,26} by a factor of 2 in order to facilitate comparisons with results from Refs. 14 and 31. An important factor in determining electronic properties of solids, off-diagonal coupling may adopt various forms^{5,21,25} other than the antisymmetric type of Eq. (6) and the symmetric type of Eq. (7). Antisymmetric coupling, for example, would be appropriate for the description of certain vibrations that promote exciton transfers between neighboring molecules when these molecules tilt toward each other, effectively decreasing the gap through which tunneling occurs. As a consequence, the tunneling between a molecule and its neighbor to the right (for example) is promoted (and tunneling on the left inhibited) when vibration tilts to the right, and tunneling on the left is promoted (and tunneling on the right inhibited) when the vibration tilts to the left. Symmetric coupling describes the circumstance in which tunneling between a molecule and its neighbors on both the left and right is promoted during the same phase of oscillation (and inhibited during the complementary phase).

Throughout this paper, we use the Fourier conventions for ladder operator c^\dagger and scalar γ as follows:

$$c_n^\dagger = N^{-\frac{1}{2}} \sum_p e^{-ipn} c_p^\dagger, \quad c_p^\dagger = N^{-\frac{1}{2}} \sum_n e^{ipn} c_n^\dagger, \quad (8)$$

$$\gamma_n = N^{-1} \sum_p e^{ipn} \gamma_p, \quad \gamma_p = \sum_n e^{-ipn} \gamma_n. \quad (9)$$

In momentum space, the tight-binding term \hat{H}^{ex} takes the form

$$\hat{H}^{\text{ex}} = -2J \sum_k a_k^\dagger a_k \cos k, \quad (10)$$

and the other terms in Eq. (1) are

$$\hat{H}^{\text{ph}} = \sum_q \omega_0 b_q^\dagger b_q, \quad (11)$$

$$\hat{H}^{\text{o.d.a}} = \frac{1}{\sqrt{N}} \sum_{kq} \omega_0 f_{-k,q}^a a_{k+q}^\dagger a_k (b_{-q}^\dagger + b_q), \quad (12)$$

$$\hat{H}^{\text{o.d.s}} = \frac{1}{\sqrt{N}} \sum_{kq} \omega_0 f_{-k,q}^s a_{k+q}^\dagger a_k (b_{-q}^\dagger + b_q), \quad (13)$$

where $f_{k,q}^a = i2\phi[\sin k - \sin(k-q)]$ and $f_{k,q}^s = 2\phi[\cos k + \cos(k-q)]$. We indicate the exciton and phonon wave vectors by Latin indices k and q , and reserve the Greek κ for the joint crystal momentum. For the latter, the operator which describes the total momentum of the exciton and the phonons can be written as

$$\hat{P} = \sum_k \kappa a_k^\dagger a_k + \sum_q q b_q^\dagger b_q. \quad (14)$$

It is noted that the crystal momentum operator \hat{P} commutes with the Hamiltonian in Eq. (1), i.e., $[\hat{P}, \hat{H}] = 0$, and therefore, the Hamiltonian \hat{H} and \hat{P} share the same set of eigenstates which are labeled by κ . By using the periodic boundary condition, the crystal momentum in the first Brillouin zone can vary from $-\pi$ to π with an increment $\delta_\kappa = 2\pi/N$.

Off-diagonal coupling was known to have significant influences on the soliton formation in long-chain polyenes, with a fundamental role in the charge-transfer doping mechanism.¹⁵ It has been shown to be of relevance for charge transport in organic semiconductors,⁴⁷ and carbon nanotubes.⁴⁸ For diagonal exciton-phonon coupling, it is well known that with increasing coupling strength, the lattice distortions induced by the exciton can trap the exciton itself. During the self-trapping process, the spatial extension of the polaron decreases while its effective mass increases. The exciton-phonon composite will change from a large polaron to a small polaron with a localized structure. Despite being a matter studied to far less degree, off-diagonal coupling is expected to lead to similar behavior perhaps with more interesting features.

III. ANTISYMMETRIC OFF-DIAGONAL COUPLING

A. Exact diagonalization procedure

It is illuminating to apply ED to investigate the Holstein model with antisymmetric off-diagonal coupling in Eq. (6), in order to explore the dependence of the polaron transitions on the lattice size and the exciton-phonon coupling strength. In the ED analysis of the Holstein model, we employ the standard Lanczos algorithm in combination with a well-controlled truncation scheme of the phononic Hilbert space. A general wave function for the Holstein Hamiltonian describing one exciton on a finite one-dimensional lattice with N sites can be written as a direct product of exciton and phonon states

$$|\varphi\rangle = \sum_{l,s} c_{l,s} |l\rangle_{\text{ex}} |s\rangle_{\text{ph}}, \quad (15)$$

where $|l\rangle_{\text{ex}} = |n_1, \dots, n_N\rangle$ ($\sum_i n_i = 1$) is the exciton state with n_i the exciton number on site i with dimension $D_{\text{ex}} = N$, and

$$|s\rangle_{\text{ph}} = \prod_{i=1}^N \frac{1}{\sqrt{m_i!}} (b_i^\dagger)^{m_i} |0\rangle_{\text{ph}} = |m_1 \dots m_N\rangle, \quad (16)$$

are the phonon states with dimension D_{ph} . It should be noted that the total dimension of Hamiltonian is $D_{\text{ex}} \times D_{\text{ph}}$. We truncate the bosonic Hilbert space by

$$\sum_i m_i \leq M, \quad (17)$$

limiting the maximal number of phonons to M . For example, with a set of $N = 3$ and $M = 3$, the possible configurations of phonon states $|n_1, n_2, n_3\rangle$ can be expressed as follows:

$$\begin{aligned} & |000\rangle, \\ & |100\rangle, |010\rangle, |001\rangle, \\ & |200\rangle, |110\rangle, |020\rangle, |101\rangle, |011\rangle, |002\rangle, \\ & |300\rangle, |210\rangle, |120\rangle, |030\rangle, |201\rangle, |111\rangle, |021\rangle, |102\rangle, |012\rangle, |003\rangle. \end{aligned}$$

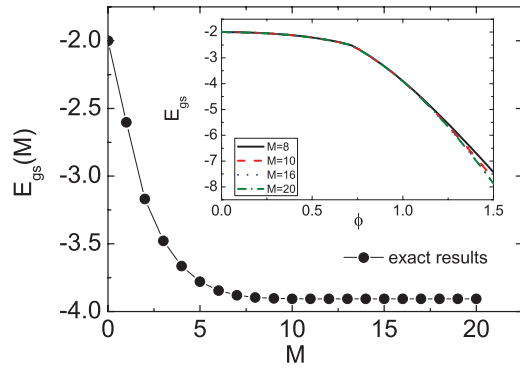


FIG. 1. Ground-state energy E_{gs} as a function of maximal number of phonons M for the Holstein model with off-diagonal coupling on a six-site lattice. The model parameters are $\phi = 1.0$, $J = 1.0$, and $\omega = 1$ (all energies are measured in units of ω). Inset: The ground-state energy E_{gs} as a function of off-diagonal coupling strength ϕ with different truncated number M .

Consequently, the total number of phonon basis states is $D_{\text{ph}} = 20$. We perform ED on small clusters up to $N = 16$ sites with the truncation number $M = 8$, yielding a phonon dimension $D_{\text{ph}} = 735471$. To reduce the dimension of the Hamiltonian matrix, we take the translational symmetry into consideration, and set the symmetrized basis as

$$|\varphi_s^{\kappa}\rangle = \frac{1}{\sqrt{N}} \sum_{i=1}^N e^{i\kappa n} T_n(|1, 0, \dots, 0\rangle \otimes |s\rangle_{\text{ph}}). \quad (18)$$

Note that the total crystal momentum of the system is

$$\kappa = 2\pi l/N, \quad (l = -N/2 + 1, \dots, N/2) \quad (19)$$

and in each κ subspace we have $D_{\text{tot}, \kappa} = D_{\text{ph}}$. T_n represents the lattice translational operator.

The resulting Hamiltonian matrix is diagonalized by the Lanczos method. As the numerical convergence of the diagonalization procedure depends on the bosonic Hilbert space, one needs to use a maximal phonon number M large enough to obtain sufficient numerical accuracy for eigenvalues. To check the convergence of the truncation procedure, the dependence of the ground-state energy E_{gs} on the maximal phonon number M is examined for a six-site lattice with antisymmetric off-diagonal coupling strength $\phi = 1.0$, and results are displayed in Fig. 1. Good convergence is found for $M \geq 10$ with a relative error less than 10^{-6} . Moreover, a larger phonon number M is needed in the strong coupling regime, as clearly shown in the inset of Fig. 1. In our calculations convergence is considered achieved if the relative error of the ground-state energy is less than 10^{-6} . The accuracy obtained in our work exceeds that reported previously in the literature.^{31,39}

We calculate the ground state energy E_{gs} for three lattice sizes $N = 6$ ($M = 16$), $N = 8$ ($M = 12$), and $N = 16$ ($M = 6$) by ED and results are shown in Fig. 2(a). The first derivative of the ground state energy with respect to the antisymmetric off-diagonal coupling strength, $\partial E/\partial\phi$, is not a continuous function of ϕ [cf. inset of Fig. 2(a)], which indicates that a phase transition may exist. We see a series of phase-transition-like discontinuities at different off-diagonal coupling strengths beyond the first critical coupling ϕ_c^0 . This behavior is ascribed

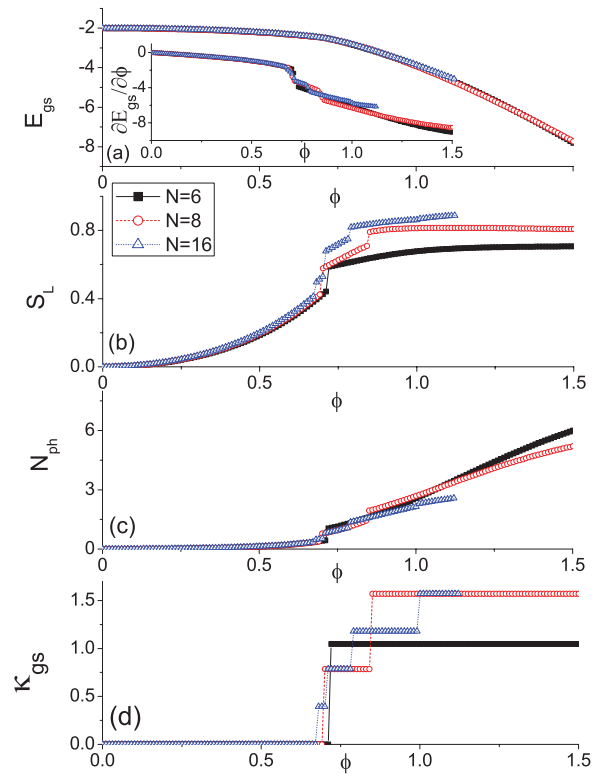


FIG. 2. (a) Ground-state energy E_{gs} , (b) the linear entropy S_L , (c) the average phonon occupation number N_{ph} , and (d) the ground-state crystal momentum κ_{gs} obtained by ED with the periodic boundary for the case of antisymmetric off-diagonal coupling for lattice size $N = 6$ ($M = 16$) (squares, only shown for $\phi < 1.2$ due to precision limitation), $N = 8$ ($M = 12$) (circles), and $N = 16$ ($M = 6$) (triangles). Inset: The first derivative of ground state energy with respect to the coupling strength ϕ , $\partial E/\partial\phi$, as a function of off-diagonal coupling ϕ . We set $\hbar = \omega = 1$.

to the nature of the intrinsic polaron properties driven by the antisymmetric off-diagonal coupling in finite-sized systems.

In order to make our discussion quantitative, we analyze the quantum entanglement between the excitonic and phononic degrees of freedom by the linearized von Neumann entropy, defined as

$$S_L = 1 - \text{Tr}_e(\rho_e)^2, \quad (20)$$

and the phonon-traced single exciton density matrix ρ_e is derived from Eq. (15)

$$\rho_e = \text{Tr}_{\text{ph}}|\varphi\rangle\langle\varphi|/\langle\varphi|\varphi\rangle, \quad (21)$$

where Tr_{ph} denotes tracing over the phonons degrees of freedom. Eq. (20) is a linearized version of the von Neumann entropy $S(\rho) = -\text{Tr}(\rho \ln \rho)$ and vanishes for a free exciton. Saturation of the linear entropy is given by the maximally mixed state for which $S_{L, \text{max}} = 1 - N^{-1}$. The linearized entanglement S_L in Eq. (20) is employed to characterize the polaron properties from the weak to strong coupling regimes, and is expected to increase with off-diagonal coupling strength and reach saturation in the strong coupling limit.

Another important quantity to evaluate for the analysis of polaronic systems is the average phonon occupation number

N_{ph} , defined as

$$N_{\text{ph}} = \sum_i \langle \varphi | b_i^\dagger b_i | \varphi \rangle. \quad (22)$$

N_{ph} is very sensitive to the off-diagonal coupling strength and increases with the coupling strength. For small ϕ , the polaron in the ground state is almost bare and $N_{\text{ph}} \approx 0$. It turns out that the phonon number, similar to the linear entropy and the ground-state energy, is an effective tool to detect transitions induced by the off-diagonal coupling. The phase transition is therefore expected at a critical coupling strength ϕ_c^0 , where N_{ph} begins to increase abruptly. Figs. 2(b) and 2(c) exhibit some abrupt changes in the linear entropy S_L and the average phonon number N_{ph} . It is confirmed that N_{ph} tends to be zero for small ϕ , and begins to increase discontinuously after it exceeds the first critical value around $\phi_c^0 = 0.7$. Both S_L and N_{ph} show phase-transition-like jumps at certain coupling strengths ϕ_c^j ($j = 1, 2, 3, \dots$) beyond ϕ_c^0 .

With an increasing off-diagonal coupling strength, the exciton size will be increasingly limited by the lattice distortion it creates, leading eventually to an off-diagonal-coupling form of the well-known polaronic self-trapping. For sufficiently large coupling strengths, the small polaron emerges, and the corresponding quantum entanglement reaches saturation.¹³ Although both diagonal and off-diagonal exciton-phonon couplings make contributions to the formation of the polaron, the off-diagonal type has more complex influences on the properties of the polaron (such as the polaron energy band). The off-diagonal coupling can boost transport and drive the ground-state energy band wider or narrower, depending on circumstances, and toward bimodal structures. Subsequent addition of diagonal coupling only reduces the bandwidth while leaving the bimodal variation intact. The bimodal structure is characterized by the nonzero crystal momentum of the ground state. Off-diagonal coupling dimerizes the lattice structure which is compared with the site-localized polaronic correlations due to diagonal coupling. Crystal momenta can only take on a set of discrete values when a small lattice with a finite number of sites is considered. The consequent discontinuous change of the crystal momentum of the ground state will lead to the abrupt changes for the linear entropy S_L and average phonon number N_{ph} .

The observed transitions are accompanied by discontinuities in the ground-state momentum κ_{gs} changing from 0 to $\pi/2$ with increments $\delta_\kappa = 2\pi/N$, as depicted in Fig. 2(d). The transition point of the linear entropy S_L and the average phonon number N_{ph} for $N = 6$ is matched by a change of κ_{gs} from 0 to $\pi/3$. In the case of $N = 8$, the first transition corresponds to a momentum jump from 0 to $\pi/4$, and the boost of κ from $\pi/4$ to $\pi/2$ is responsible for the second transition of the entropy S_L and the average phonon number N_{ph} . For $N = 16$ there are five transition points which correspond to $\kappa = 0, \pi/8, \pi/4, 3\pi/8, \text{ and } \pi/2$, respectively. These κ -dependent crossovers, in the presence of the off-diagonal coupling, illustrate discontinuous changes in polaron properties which become more pronounced for small lattice sizes. With increasing lattice size, especially in the thermodynamic limit, there will be infinitesimal step sizes in the change of the crystal momentum if the coupling strength exceeds the first critical

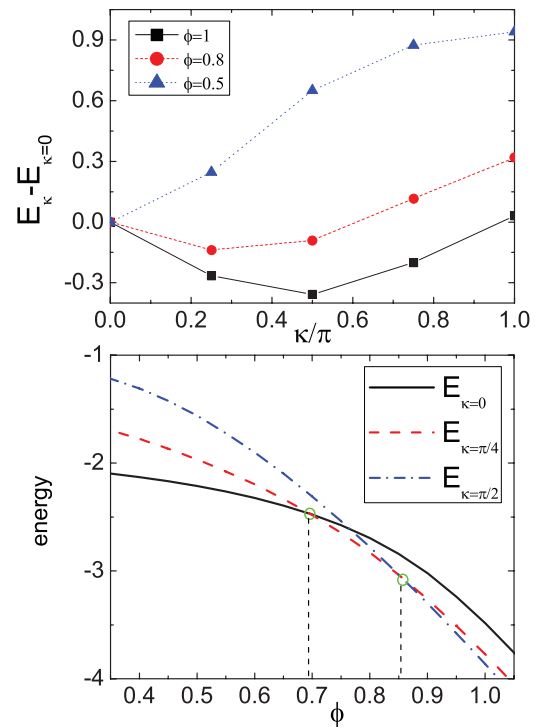


FIG. 3. (a) Polaron energy band $E_\kappa - E_{\kappa=0}$ obtained by ED for an eight-site lattice for different coupling strengths $\phi = 0.5, 0.8, \text{ and } 1$. (b) E_κ as a function of off-diagonal coupling strength ϕ for three values of the crystal momentum $\kappa = 0, \pi/4, \pi/2$. The circles are the crossing points of energy level.

point ϕ_c^0 , and all jump points will merge. As a consequence, the phase-transition-like shifts in the crystal momentum disappear. It is believed that the transition only occurs at the first critical point ϕ_c^0 which corresponds to the crystal momentum of the ground-state changing from zero to nonzero, consistent with results for the SSH model.¹⁴

In Fig. 3(a), polaron energy band $E_\kappa - E_0$ for an eight-site lattice obtained by ED is shown for three values of the off-diagonal coupling strength $\phi = 0.5, 0.8, \text{ and } 1$. The ground-state energy is found at crystal momenta $\kappa = 0, \pi/4, \text{ and } \pi/2$ for $\phi = 0.5, 0.8, \text{ and } 1$, respectively. With increasing ϕ , the ground-state crystal momentum will change from zero to $\pi/2$ by a minimal step size of $\delta_\kappa = 2\pi/N$. It is helpful to look into the κ -dependency of the ground-state energy as a function of off-diagonal coupling strength. In Fig. 3(b), the ground state energy $E_\kappa(\phi)$ is plotted for three values of the crystal momentum $\kappa = 0, \pi/4, \pi/2$. One can readily observe the energy-level-crossing which occurs at two discrete points as marked by vertical dashed lines corresponding to the critical transition coupling strengths. The presence of the transition phenomenon is due to the fact that it is not possible to have a smooth transition from the zero momentum state into states with finite momenta. This is strikingly different from the diagonal coupling case where the ground-state crystal momentum is always zero regardless of the diagonal coupling strength.

To probe the influence of the periodic boundary (PB) condition, we study the ground state energy E_{gs} and the linear entropy S_L with the open boundary (OB) condition and compare results with those obtained with the PB condition. Fig. 4(a) clearly demonstrates that the OB

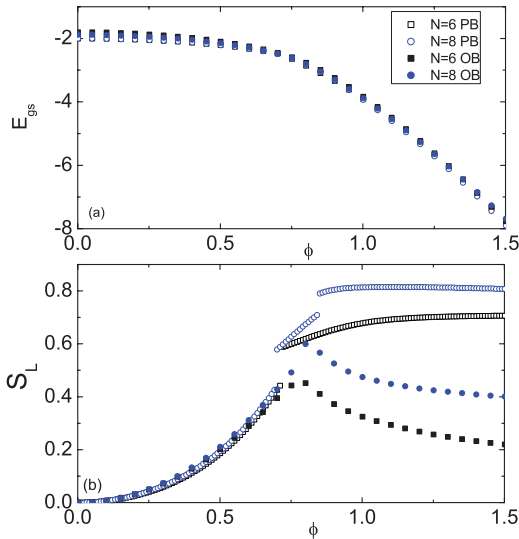


FIG. 4. (a) Ground-state energy E_{gs} and (b) the linear entropy S_L obtained by ED with the periodic boundary (PB) condition (open squares, $N = 6$; open circles, $N = 8$) and its comparison with the open boundary (OB) condition (solid squares, $N = 6$; solid circles, $N = 8$). It is observed that the discontinuous transitions vanish under the OB condition.

ground-state energy is higher than the PB counterpart. The distinction between the two boundary conditions becomes apparent in Fig. 4(b) which compares S_L from the two approaches. Under the OB condition, a cusp forms at a critical value ϕ_c^0 , while under the PB condition, there are several discontinuities at critical coupling values ϕ_c^j . This is explained by the fact that quantization of the crystal momentum is absent under the OB condition. Thus, it is shown that the existence of the abrupt transition points ϕ_c^j depends on finite-size effects and boundary conditions.

B. Variational approach

Although ED is an effective apparatus to investigate polaron properties with high accuracy, its applicability is limited to small clusters. In the strong coupling regime, especially, more phonons should be considered, and therefore, much more computing resources would be required due to an expanded phonon Hilbert space. The variational method provides a reliable alternative to complement ED for large clusters or in the strong coupling regime. In order to investigate phase-transition-like discontinuities in large clusters, the Toyozawa Ansatz is used in this subsection to deal with the Holstein model of Eq. (1) in the absence of diagonal exciton-phonon coupling.⁵ The main goal of the variational approach is to achieve, for any given crystal momentum κ , the energy minimum E_κ , which is defined as

$$E_\kappa = \langle \Psi(\kappa) | \hat{H} | \Psi(\kappa) \rangle, \quad (23)$$

where $|\Psi(\kappa)\rangle$ is an appropriately normalized delocalized trial state, and \hat{H} is the system Hamiltonian given by Eq. (1). It should be noted that the crystal momentum operator commutes with the system Hamiltonian, so the energy eigenstates are also eigenfunctions of the crystal momentum. Therefore, variations for different κ can be carried out independently (see the Appendix). The set of E_κ constitutes a variational estimate

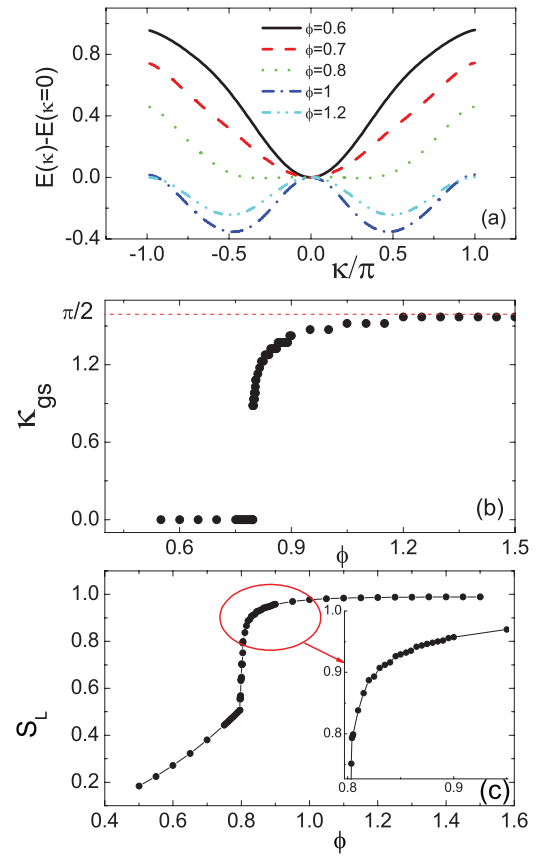


FIG. 5. (a) The polaron energy band $E_\kappa - E_{\kappa=0}$ calculated by the Toyozawa Ansatz for a range of $\phi = 0.6$ (solid line), 0.7 (dashed line), 0.8 (dotted line), 1 (dashed-dotted line), and 1.2 (dashed-dotted-dotted line); (b) the total momentum κ_{gs} of the ground state energy as a function of ϕ ; (c) the linear entropy S_L as a function of ϕ calculated by the Toyozawa Ansatz for $N = 128$ sites (see the inset for the range of ϕ from 0.8 to 1). The parameters chosen are $J = 1$, $g = 0$.

(an upper bound) for the polaron energy band.^{29,49} After the variational procedure, one can obtain the trial states which are approximations to the energy eigenstates, and as a result, the reduced density matrix can be computed as

$$\rho_{mn} = \langle \Psi(\kappa) | a_n^\dagger a_m | \Psi(\kappa) \rangle. \quad (24)$$

One can then proceed to compute the linear entropy of Eq. (20).

The trial state used in this work, Toyozawa Ansatz, reads

$$|\Psi(\kappa)\rangle = |\kappa\rangle \langle \kappa | \kappa \rangle^{-1/2}, \quad (25)$$

$$|\kappa\rangle = \sum_n e^{i\kappa n} \sum_{n_1} \alpha_{n_1-n}^\kappa a_{n_1}^\dagger \times \exp\left(-\sum_{n_2} (\beta_{n_2-n}^\kappa b_{n_2}^\dagger - \beta_{n_2-n}^{\kappa*} b_{n_2})\right) |0\rangle, \quad (26)$$

where $|0\rangle$ is the product of the exciton and phonon vacuum states, α_n^κ is the exciton amplitude and β_n^κ is the phonon displacement.

The polaron energy bands calculated by the Toyozawa Ansatz with lattice size up to $N = 128$ are shown in Fig. 5(a), from which it is obvious that the ground state energy is

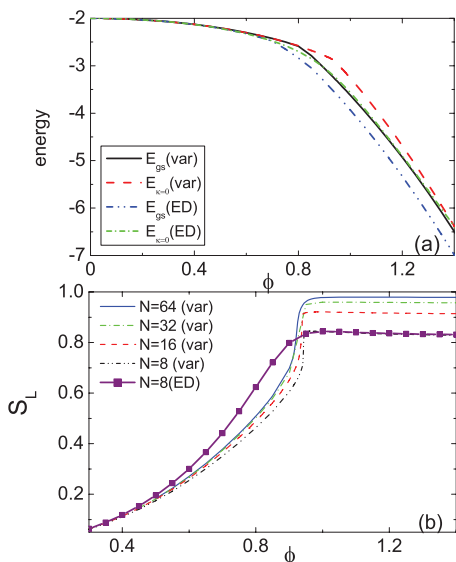


FIG. 6. (a) Using ED and the variational method (var), the ground state energy E_{gs} is compared with $E_{\kappa=0}$ for an eight-site lattice. (b) The linear entropy S_L at $\kappa = 0$ calculated by the variational method for lattice sizes $N = 8$ (dashed-double-dotted line), 16 (dashed line), 32 (dashed-dotted line), and 64 (solid line) with its comparison to that obtained by ED for eight-site lattice (squares). It indicates that there is a smooth transition from large to small polaron zone at zero momentum.

achieved at the crystal momentum $\kappa = 0$ if the off-diagonal coupling ϕ is very small. However, a bimodal variation will appear when ϕ is large enough, and the crystal momentum κ at which minimum of polaron energy will be achieved in leaps from 0 to $\pm\pi/2$.²⁵ The crystal momentum κ corresponding to the ground state energy as a function of ϕ is shown in Fig. 5(b). One sees immediately that there are many critical coupling values ϕ_c^j at which the crystal momentum κ changes from zero to $\pi/2$ with the interval value $2\pi/N$. Due to the remarkable expansion of the lattice size the Toyozawa Ansatz is able to handle (compared with ED), the increments of the ground-state crystal momentum κ will be much smaller, leading to a smooth transition except for the first critical coupling strength. In the limit of infinite lattice size, there exists a sharp transition at the first critical point ϕ_c^0 , and other jump points disappear.

The quantum entanglement S_L between the excitonic and phononic degrees of freedom calculated by the Toyozawa Ansatz for $N = 128$ is shown in Fig. 5(c). It is clear that the quantum entanglement of the large cluster is much smoother than that of the small cluster calculated by ED. However, more jumps, corresponding to the critical coupling strengths, emerge with smaller jump amplitudes as shown in the inset of Fig. 5(c). Due to the increase of the lattice size, the ground-state crystal momentum is allowed to take more distinct values, and can change from zero to finite values with much smaller steps as the strength of antisymmetric off-diagonal coupling is increased. It should be noted that the first critical coupling strength is quite different from the others, as it remains conspicuous for very large aggregates. With the exception of the first critical coupling strength ϕ_c^0 , other critical values of the coupling parameter ϕ_c^j ($j \neq 0$) are expected to vanish as $N \rightarrow \infty$.

Although the ground state is not always found at $\kappa = 0$ as the antisymmetric off-diagonal coupling ϕ is varied, it is still interesting to compare the ground state energy with $E_{\kappa=0}$. Fig. 6(a) shows that the ground state energy of an eight-site lattice calculated by both ED and the Toyozawa Ansatz is much lower than that $E_{\kappa=0}$. It indicates that the energy at the zero crystal momentum is not always the ground-state energy, an important fact that was not addressed in Ref. 31. We also plot the entanglement between the excitonic and phononic degrees of freedom at $\kappa = 0$ in Fig. 6(b). The linear entropy calculated by ED for lattice size $N = 8$ is a smooth function with the increasing of ϕ . On the other hand, the variational results also exhibit a smoothly varying linear entropy as the lattice size increases. It should be noted that the linear entropies calculated by the Toyozawa Ansatz and ED are not entirely consistent in the intermediate coupling regime for the lattice size $N = 8$ as shown in Fig. 6(b). The difference is attributed to the insufficient complexity of the Toyozawa Ansatz which limits its accuracies in this regime. The phonon displacement $\beta_{n_2-n}^k$ of the Toyozawa Ansatz mainly depends on the position of the phonon n_2 , while it can hardly reflect the influences of the exciton on the lattice deformation. In the intermediate coupling regime, the formation of the phonon cloud has close relations with the electronic excitation, which leads to the unsatisfactory performances of the Toyozawa Ansatz in this regime.

Compared with the Toyozawa Ansatz, an additional array is added to the phonon displacement parameters in the Global-Local Ansatz, which captures the influence of the exciton on the phonon displacement and depends on the relative distance between the exciton and phonon. A more general form of the phonon displacements using an $N \times N$ matrix instead of one or two arrays of size N is introduced in the delocalized D_1 Ansatz. The Global-Local Ansatz and the delocalized D_1 Ansatz, both sophisticated variants of the Toyozawa Ansatz, are believed to be capable to deliver more accurate results as they include explicit correlations between the electronic excitation and the phonon displacements.²⁷ A combination of the ED and variational trial states such as the Toyozawa Ansatz enables us to obtain significantly more reliable results compared with those in the existing literature,³¹ revealing a smooth crossover from weak coupling to strong coupling regimes for the zero crystal momentum.

IV. SYMMETRIC OFF-DIAGONAL COUPLING

Since we have shown that the presence of the antisymmetric off-diagonal coupling leads to a phase-transition-like behavior, it is a natural question to ask whether this behavior is attributed to the symmetry of the off-diagonal coupling, and whether symmetric off-diagonal coupling has the same effect. Although the expressions of the antisymmetric and symmetric off-diagonal exciton-phonon couplings appear similar, they have different influences on the properties of the polaron. For example, the antisymmetric off-diagonal coupling promotes exciton transfers between neighboring molecules tilted toward each other. For the symmetric coupling, tunneling between a molecule and its neighbors on both the left and right sides is promoted during the same phase of oscillation.

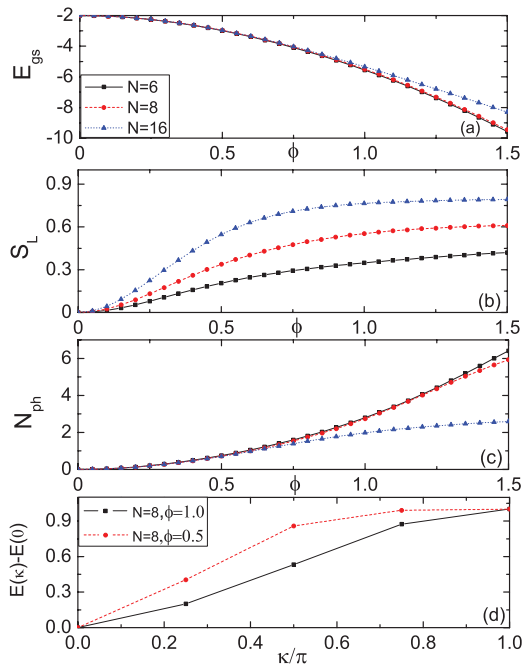


FIG. 7. (a) Ground-state energy E_{gs} , (b) the linear von Neumann entropy S_L , and (c) the average phonon occupation number N_{ph} in the ground state obtained by ED as a function of the symmetric off-diagonal coupling ϕ for lattice size $N = 6$ ($M = 16$) (solid line and squares), $N = 8$ ($M = 12$) (dashed line and circles), and $N = 16$ ($M = 6$) (dotted line and triangles). (d) The corresponding polaronic band dispersion $E_{\kappa} - E_{\kappa=0}$ for $N = 8$ lattices obtained by ED.

We now discuss the polaron properties for the case of symmetric off-diagonal coupling in Eq. (7). The ground-state energy E_{gs} , the quantum entropy S_L between the excitonic and phononic degrees of freedom, and the average phonon number N_{ph} of the ground state are plotted in Fig. 7 for lattice sizes $N = 6, 8$, and 16 using ED. All curves appear smoothly varying as the symmetric off-diagonal coupling strength ϕ is increased. In Fig. 7(d), the polaron energy dispersion $E_{\kappa} - E_{\kappa=0}$ is displayed for an eight-site lattice and two values of the coupling strength ϕ . As expected, the ground-state energy is found at the Brillouin zone center $\kappa = 0$ for both cases (weak coupling $\phi = 0.5$ and strong coupling $\phi = 1$). The fact that the polaron band minimum is always located at zero crystal momentum for all coupling strengths leads to the conclusion that there is a smooth crossover for symmetric off-diagonal coupling (similar to the case of diagonal coupling).

V. CONCLUSION

In this paper, we have examined polaronic discontinuities induced by off-diagonal exciton-phonon coupling in the Holstein model. Two approaches, ED and a variational method using the Toyozawa Ansatz, have been adopted to probe the ground state properties of the Holstein polaron. Compared with previous ED treatments of the Holstein model, we are able to deal with much larger clusters by means of Lanczos diagonalization with translational symmetry. Larger lattice sizes are essential for a thorough analysis of finite-size effects and phase-transition-like properties for the case of antisymmetric off-diagonal coupling, a subject of recent controversy. For

lattice sizes over 16, we have used an efficient, yet quite accurate variational treatment based on the Toyozawa Ansatz. The Toyozawa Ansatz can deal with much larger clusters with less computing resources despite that its accuracy may not be satisfactory in the weak coupling regime and for small clusters. In addition, the Toyozawa Ansatz does not use the truncation of the phonon Hilbert space, a substantial source of deficiency of ED in the strong coupling regime. Given the mounting interest in quantum entanglement, which is often a telltale signature of phase transitions, we have used linearized von Neumann entropy to quantify the exciton-phonon correlations in Holstein polaron. The average phonon occupation number has also been employed to analyze the influence of the off-diagonal exciton-phonon coupling.

When only antisymmetric exciton-phonon coupling is present, the ground state is found to possess zero crystal momentum for weak coupling but finite crystal momenta for strong coupling. Both the ground-state entanglement and the average phonon occupation number display discontinuities when the coupling strength exceeds the first critical value ϕ_c^0 . Additional critical coupling strengths ϕ_c^j also exist for small lattice sizes with the PB condition. However, if we apply the OB condition to the same clusters, only ϕ_c^0 exists. The boundary condition will limit the crystal momenta to some discrete values which have the same number with the lattice size. To further probe the effect of the lattice size and the boundary condition, the Toyozawa Ansatz is employed to treat large clusters. More discontinuous jumps of the ground-state linear entropy are shown to emerge, but the amplitudes of the jumps are much reduced except for the one at ϕ_c^0 . Therefore, it is expected that the only surviving discontinuity in the linear entropy in the thermodynamic limit $N \rightarrow \infty$ will be one at the first critical coupling strength ϕ_c^0 .

We have also studied the entanglement between the excitonic and phononic degrees of freedom at the Brillouin zone center (rather than that of the ground state). In this case, the linear entropies of the small clusters calculated by ED, as well as the large clusters calculated by Toyozawa, show a smooth crossover between weak and strong coupling regimes. It indicates that no phase transitions exist at the Brillouin zone center. Finally, the effect of the symmetric off-diagonal exciton-phonon coupling has been examined. No phase-transition-like behavior is found in the presence of the symmetric coupling. The ground-state energy is always achieved at the Brillouin zone center for all parameter regimes.

ACKNOWLEDGMENTS

Support from the Singapore National Research Foundation through the Competitive Research Programme (CRP) under Project No. NRF-CRP5-2009-04 and the Singapore Ministry of Education through the Academic Research Fund (Tier 2) under Project No. T207B1214 is gratefully acknowledged.

APPENDIX: TOYOZAWA ANSATZ

The Toyozawa Ansatz may be viewed as a time-independent translationally invariant rendering of the

so-called Davydov's D_2 Ansatz state underlying much of the theory of the Davydov soliton,^{24,29}

$$|D_2\rangle = |\alpha\rangle \otimes |\beta\rangle, \quad (\text{A1})$$

where \otimes denotes the direct product, $|\alpha\rangle$ and $|\beta\rangle$ are the exciton and phonon parts of the localized state respectively, built as follows:

$$|\alpha\rangle = \sum_n \alpha_n a_n^\dagger |0\rangle_{\text{ex}}, \quad (\text{A2})$$

$$|\beta\rangle = \exp\left[-\sum_m (\beta_m b_m^\dagger - \beta_m^* b_m)\right] |0\rangle_{\text{ph}}, \quad (\text{A3})$$

where α_n is the exciton amplitude, β_m is the phonon displacement, $|0\rangle_{\text{ex}}$ and $|0\rangle_{\text{ph}}$ are the exciton and phonon vacuum states respectively. For D_2 Ansatz, the typically pulse-shaped distribution of the displacements β_n describes a lattice deformation fixed in the frame of the lattice, to which conforms a correspondingly pulse-shaped distribution of exciton probability amplitudes α_n .⁵

D_2 Ansatz can be delocalized into the Toyozawa Ansatz via a projection operator \hat{P}^κ ,

$$\hat{P}^\kappa = N^{-1} \sum_n e^{i(\kappa - \hat{P})n} = \delta(\kappa - \hat{P}), \quad (\text{A4})$$

where $\hat{P} = \sum_k k a_k^\dagger a_k + \sum_q q b_q^\dagger b_q$. After the delocalization, the site-space representation of the Toyozawa Ansatz is given by

$$|\kappa\rangle = \sum_n e^{i\kappa n} \sum_{n_1} \alpha_{n_1-n}^\kappa a_{n_1}^\dagger \times \exp\left(-\sum_{n_2} (\beta_{n_2-n}^\kappa b_{n_2}^\dagger - \beta_{n_2-n}^{\kappa*} b_{n_2})\right) |0\rangle, \quad (\text{A5})$$

where $|0\rangle = |0\rangle_{\text{ex}} \otimes |0\rangle_{\text{ph}}$ is the vacuum state for both the exciton and phonon fields. Applying the Fourier conventions, we can get the Toyozawa Ansatz in the momentum-space representation easily,

$$|\kappa\rangle = N^{-1/2} \sum_{nk} e^{i(\kappa-k)n} \alpha_k^\kappa a_k^\dagger \times \exp\left(-N^{-1/2} \sum_q (\beta_q^\kappa e^{-iqn} b_q^\dagger - \beta_q^{\kappa*} e^{iqn} b_q)\right) |0\rangle. \quad (\text{A6})$$

It should be noted that $|\kappa\rangle$ is not normalized, but few modifications are needed to change it into normalized one as $|\Psi(\kappa)\rangle = |\kappa\rangle \langle \kappa | \kappa \rangle^{-1/2}$.

¹V. Vedral, *Nature (London)* **425**, 28 (2003); *New J. Phys.* **6**, 102 (2004).

²G. De Chiara, Č. Brukner, R. Fazio, G. M. Palma, and V. Vedral, *New J. Phys.* **8**, 95 (2006).

³T. Holstein, *Ann. Phys. (N.Y.)* **8**, 325 (1959); 343 (1959).

⁴H. de Raedt and A. Lagendijk, *Phys. Rev. B* **27**, 6097 (1983); **30**, 1671 (1984).

⁵Y. Zhao, D. W. Brown, and K. Lindenberg, *J. Chem. Phys.* **107**, 3159 (1997); **3179** (1997); **106**, 5622 (1997); A. Romero, D. W. Brown, and K. Lindenberg, *ibid.* **109**, 6540 (1998).

⁶P. E. Kornilovitch, *Phys. Rev. Lett.* **81**, 5382 (1998).

⁷E. V. L. de Mello and J. Ranninger, *Phys. Rev. B* **55**, 14872 (1997).

⁸A. S. Alexandrov, V. V. Kabanov, and D. K. Ray, *Phys. Rev. B* **49**, 9915 (1994).

⁹E. Jeckelmann and S. R. White, *Phys. Rev. B* **57**, 6376 (1998).

¹⁰S. R. White, *Phys. Rev. B* **48**, 10345 (1993).

¹¹V. Cataudella, G. De Filippis, and G. Iadonosi, *Phys. Rev. B* **60**, 15163 (1999); **62**, 1496 (2000).

¹²J. Bonca, S. A. Trugman, and I. Batistić, *Phys. Rev. B* **60**, 1633 (1999).

¹³Y. Zhao, P. Zanardi, and G. H. Chen, *Phys. Rev. B* **70**, 195113 (2004); J. Sun, Y. Zhao, and W. Z. Liang, *ibid.* **79**, 155112 (2009).

¹⁴D. J. J. Marchand *et al.*, *Phys. Rev. Lett.* **105**, 266605 (2010).

¹⁵W. P. Su, J. R. Schrieffer, and A. J. Heeger, *Phys. Rev. Lett.* **42**, 1698 (1979); *Phys. Rev. B* **22**, 2099 (1980).

¹⁶J. Zaanen and P. B. Littlewood, *Phys. Rev. B* **50**, 7222 (1994).

¹⁷K. Yonemitsu and N. Maeshima, *Phys. Rev. B* **76**, 075105 (2007).

¹⁸L. A. Dissado and S. H. Walmsley, *Chem. Phys.* **86**, 375 (1984).

¹⁹H. Sumi, *Chem. Phys.* **130**, 433 (1989).

²⁰A. S. Mishchenko and N. Nagaosa, *Phys. Rev. Lett.* **86**, 4624 (2001).

²¹S. Ishihara and N. Nagaosa, *Phys. Rev. B* **69**, 144520 (2004).

²²L. D. Landau, *Phys. Z. Sowjetunion* **3**, 644 (1933).

²³G. D. Mahan, *Many-Particle Physics* (Kluwer Academic/Plenum, New York, 2000).

²⁴Y. Zhao, Doctoral thesis, University of California, San Diego, 1994.

²⁵Y. Zhao, D. W. Brown, and K. Lindenberg, *J. Chem. Phys.* **100**, 2335 (1994).

²⁶Y. Zhao, D. W. Brown, and K. Lindenberg, *J. Chem. Phys.* **106**, 2728 (1997).

²⁷Y. Zhao, G. Q. Li, J. Sun, and W. H. Wang, *J. Chem. Phys.* **129**, 124114 (2008).

²⁸R. W. Munn and R. Silbey, *J. Chem. Phys.* **83**, 1843 (1985); **1854** (1985).

²⁹Y. Toyozawa, *Prog. Theor. Phys.* **26**, 29 (1961).

³⁰Q. M. Liu, Y. Zhao, W. H. Wang, and T. Kato, *Phys. Rev. B* **79**, 165105 (2009).

³¹V. M. Stojanović and M. Vanević, *Phys. Rev. B* **78**, 214301 (2008).

³²Y. Y. Zhang, *et al.*, *J. Phys.: Condens. Matter* **21**, 415601 (2009); *Solid State Commun.* **149**, 2106 (2009).

³³S. Sachdev, *Quantum Phase Transitions* (Cambridge University Press, 1999).

³⁴N. Lambert, C. Emary, and T. Brandes, *Phys. Rev. Lett.* **92**, 073602 (2004); *Phys. Rev. A* **71**, 053804 (2005); S. J. Gu, H. Q. Lin, and Y. Q. Li, *ibid.* **68**, 042330 (2003).

³⁵W. K. Wootters, *Phys. Rev. Lett.* **80**, 2245 (1998).

³⁶H. Fehske, *Spin Dynamics, Charge Transport and Electron-Phonon Coupling Effects in Strongly Correlated Electron Systems* (Universität Bayreuth, Habilitationsschrift, 1996).

³⁷A. Alvermann, H. Fehske, and S. A. Trugman, *Phys. Rev. B* **81**, 165113 (2010).

³⁸J. Bonča, S. A. Trugman, and I. Batistić, *Phys. Rev. B* **60**, 1633 (1999).

³⁹C. A. Perroni, E. Piegari, M. Capone, and V. Cataudella, *Phys. Rev. B* **69**, 174301 (2004).

⁴⁰Q. H. Chen, Y. Y. Zhang, T. Liu, and K. L. Wang, *Phys. Rev. A* **78**, 051801(R) (2008); Y. Y. Zhang, Q. H. Chen, and K. L. Wang, *Phys. Rev. B* **81**, 121105(R) (2010).

⁴¹Y. Zhao and H. N. Bertram, *J. Magn. Magn. Mater.* **114**, 329 (1992).

⁴²Y. Zhao, and H. N. Bertram, *J. Appl. Phys.* **77**, 6411 (1995); B. Yang and Y. Zhao, *ibid.* **110**, 103908 (2011).

⁴³M. Capone, W. Stephan, and M. Grilli, *Phys. Rev. B* **56**, 4484 (1997).

⁴⁴J. Bonca, S. A. Trugman, and I. Batistić, *Phys. Rev. B* **60**, 1633 (1999).

⁴⁵R. E. Lagos and R. A. Friesner, *Phys. Rev. B* **29**, 3045 (1984).

⁴⁶E. O. Potma and D. A. Wiersma, *J. Chem. Phys.* **108**, 4894 (1998).

⁴⁷A. Troisi and G. Orlandi, *Phys. Rev. Lett.* **96**, 086601 (2006); H. Ding *et al.*, *Appl. Phys. Lett.* **96**, 222106 (2010).

⁴⁸L. E. F. Foa Torres and S. Roche, *Phys. Rev. Lett.* **97**, 076804 (2006).

⁴⁹T. D. Lee, F. E. Low, and D. Pines, *Phys. Rev.* **90**, 297 (1953).